FACULDADE DE ENGENHARIA DA UNIVERSIDADE DO PORTO

ns-3 Simulation Model for Underground Networks

Sérgio Davide Lopes Conceição

Master in Electrical and Computers Engineering

Supervisor: Manuel Alberto Pereira Ricardo (PhD)

Co-supervisor: Filipe Ribeiro (MSc)

June, 2014

U.PORTO
FEUP FACULDADE DE ENGENHARIA UNIVERSIDADE DO PORTO

MIEEC - MESTRADO INTEGRADO EM ENGENHARIA ELETROTÉCNICA E DE COMPUTADORES 2013/2014

A Dissertação intitulada

"ns-3 Smulation Model for Underground Networks"

foi aprovada em provas realizadas em 15-07-2014

o júri

Presidente Professor Doutor Sílvio Almeida Abrantes Moreira
Professor Auxiliar do Departamento de Engenharia Eletrotécnica e de Computadores da Faculdade de Engenharia da Universidade do Porto

Professor Doutor Jorge Botelho da Costa Mamede
Professor Adjunto do Departamento de Engenharia Eletrotécnica do Instituto Superior de Engenharia do Porto

Professor Doutor Manuel Alberto Pereira Ricardo
Professor Associado do Departamento de Engenharia Eletrotécnica e de Computadores da Faculdade de Engenharia da Universidade do Porto

O autor declara que a presente dissertação (ou relatório de projeto) é da sua exclusiva autoria e foi escrita sem qualquer apoio externo não explicitamente autorizado. Os resultados, ideias, parágrafos, ou outros extratos tomados de ou inspirados em trabalhos de outros autores, e demais referências bibliográficas usadas, são corretamente citados.

Autor - Sérgio Davide Lopes Conceição

Faculdade de Engenharia da Universidade do Porto

Abstract

Underground communications networks have many interesting applications such as border surveillance, agriculture monitoring and infrastructure monitoring. The first networks used in these applications were wired networks, but recent studies have shown that wireless underground networks are feasible and have deployment advantages.

Wireless underground networks can have nodes buried in the soil, which establish communication between them or have some nodes aboveground as data sinks; in the later case, the communication is between aboveground and underground devices. This dissertation addresses the need for a simulation environment for these networks and accomplishes that need by implementing this environment into the network simulator ns-3. Further the results obtained are also validated using experiments done previously in the field for the 433 MHz and 2.4 GHz frequencies. The results obtained regarding the accuracy of the model revealed to be quite promising, which may lead to attract more investigators into this particular field of study.

Acknowledgments

I would like to thank to my advisor Prof Manuel Ricardo, for giving be the opportunity of doing this research project. Also, to my co-advisor, Filipe Ribeiro, for his full support, help to overcome some challenges that we faced and for some of his great ideas that made this work as it is. I also thank Dr Rui Campos for all the support and suggestions during the realization of this work, because although he was not an official supervisor he assisted me right from the beginning of this work.

I also thank to my friends for all the support during, not only this work, but also during all the course. Finally I thank to my parents and my brother for all the support during my whole life.

The author would like to thank the BEST CASE project (“NORTE-07-0124-FEDER-000058" and “NORTE-07-0124-FEDER-000060") financed by the North Portugal Regional Operational Programme (ON.2 – O Novo Norte), under the National Strategic Reference Framework (NSRF), through the European Regional Development Fund (ERDF), and by national funds, through the Portuguese funding agency, Fundação para a Ciência e a Tecnologia (FCT).

Sérgio Conceição

"I have not failed.
I've just found 10,000 ways that won't work."

Thomas A. Edison

Contents

List of Figures

List of Tables

Acronyms

A2U	Aboveground-to-underground
AODV	Ad hoc On-Demand Distance Vector
DSS	Direct Spread Spectrum
EM	Electromagnetic
FEC	Forward Error Correction
GRMDM	Generalized refractive mixing dielectric model
LTE	Long Term Evolution
MAC	Medium Access Control
MBSDM	Mineralogy-based soil dielectric model
MI	Magnetic Induction
MSc	Master of Science
Ns-3	Network simulator 3
OFDM	Orthogonal Frequency Division Multiplexing
OLSR	Optimized Link State Routing Protocol
OTA	Over-the-Air
PLR	Packet Loss Ratio
RTT	Round-Trip Time
SMDM	Semi-empirical dielectric model
TCP	Transmission Control Protocol
U2A	Underground-to-aboveground
U2U	Underground-to-underground
UDP	User Datagram Protocol
WiMax	Worldwide Interoperability for Microwave Access
WSN	Wireless Sensor Network
WUN	Wireless Underground Network
WUSN	Wireless Underground Sensor Network

Chapter 1

Introduction

1.1 Context

Underground communications are common in mines and tunnels. In the past years the research work has been increasing in this area. Although these scenarios are different from the aboveground over-the-air (OTA) communications, the propagation medium is still the air. Wireless communications through soil with applications such as agriculture and maintenance of playing fields are an emerging topic. Since this type of communications involve using the soil as the propagation medium, new propagation models have to be created and new challenges have to be addressed. The soil is characterized by several properties that we need to take into account, such as texture and water content. In particular, the water content is a property that depends on the weather and so it can vary from low water content in a sunny day to high water content in a rainy day.

A wireless underground network typically includes underground and aboveground nodes, as we can see in the Figure 1.1

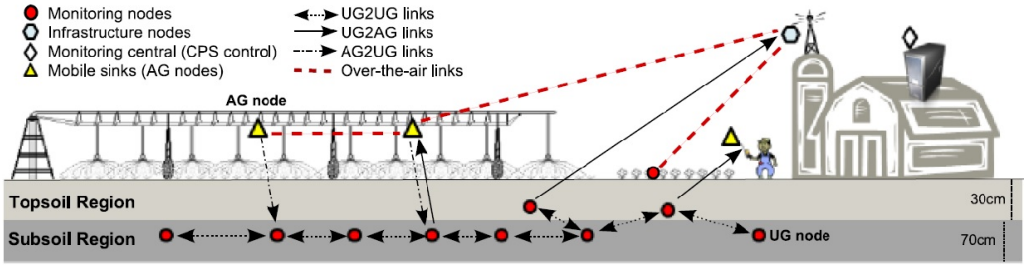

Figure 1.1: Example of a wireless underground network with aboveground and underground nodes. [1]

Although there is significant research work produced in the last years, wireless underground networks are an emerging topic and there are still many challenges and problems to be addressed.

1.2 Motivation

A number of research works have been made in the past few years regarding wireless underground communications because they revealed to be a good alternative to wired solutions. However, because the propagation medium is the soil, the communications conditions vary regarding its characteristics which are highly weather dependent. For example, in a rainy day the quantity of water in the soil increases changing its propagation characteristics.

In order to overcome the difficulties to design a network of this type we need to be able to simulate the target network for several scenarios. Then, with the results we can determine, for example, the minimum distance between nodes that can guarantee connectivity between nodes for different amounts of water in the soil. Also, before doing field experiments with new wireless underground networking solutions they need to be evaluated in simulations, for an easier control of the tests.

The ns-3 is the simulator chosen for implement the simulation environment for underground networks because it is widely used by the research community including our research group. This implementation in a network simulator is an important contribution to develop new networking solutions for this environment and also for research purposes.

1.3 Objectives

The goal of this dissertation is to develop a new simulation model for ns-3 that allows simulation of wireless underground networks for different frequencies, types of soils and depths of the nodes. The ns-3 model has to be able to simulate communications between only buried nodes or between buried nodes and aboveground nodes. To achieve this goal the work was divided into some specific objectives:

- Study the major properties characterizing the soil and models;
- Study some experiments and the existing radio propagation models for underground networks;
- Study the ns-3 simulation environment, in particular the methodology that shall be used to implement and add new models to the simulator;
- Implement the propagation models in ns-3;
- Simulate the same experimental scenarios found in literature and compare the obtained results with the documented ones;
- Conclude about the accuracy of the implemented wireless underground simulation environment.

1.4 Document Structure

This document is organized in five chapters. Chapter 2 presents the state of the art in Wireless Underground Networks (WUN) and the ns-3 network simulator. Chapter 3 shows the methodology used to achieve the goals described in this chapter. Chapter 4 presents the results obtained from our simulation framework. Finally, Chapter 5 draws the major conclusions.

Chapter 2

State of the art

In this chapter we present the state of the art on wireless underground networks. We start by defining some concepts about these networks and to point out some recent applications. Then, we present the major radio propagation models in underground networks, and also models that estimate the soil dielectric constant. We also make an introduction to magnetic induction propagation techniques and wireless networks in tunnels and caves since they are context related. Next, we present the ns-3 network simulator, since it will be the simulator used as a basis to develop the simulation environment for WUNs, and we discuss some important aspects of ns-3 in order to justify its use. Finally, we discuss the major topics presented in this chapter.

2.1 Wireless Underground Networks

Wireless Underground Networks (WUN) are networks in which some or all the nodes are located underground and use some wireless technology to communicate with each other. The communication medium is the soil or hybrid (soil plus air) when some of the nodes are located aboveground.

Since the medium in WUNs is different from the traditional wireless networks it requires the definition of new propagation models, which have been proposed in the past few years. This type of networks are mainly implemented with sensors that are monitoring some variable or process. For this reason they are also called Wireless Underground Sensor Networks (WUSN) because they are an extension of the traditional Wireless Sensor Networks (WSN) [12]. There are several applications of WUSNs to improve some sort of monitoring [13]:

- **Agriculture** — sensors can be used to monitor the soil parameters, such as water content, mineral content, salinity, and temperature, and then communicate these values in real time to a control station aboveground, in order to have soil parameters in optimal values. This type of monitoring can also be used in sports fields;
- **Security** — sensors buried at a shallow depth can detect movement at the surface. This is useful for home security as well as military applications such as border patrol. Although

these tasks can be done with aboveground sensors they benefit if they are underground since in this case they remain hidden;

- **Infrastructure Monitoring** — a WUN can be used to monitor underground plumbing leakage as well as electrical and communication wiring.

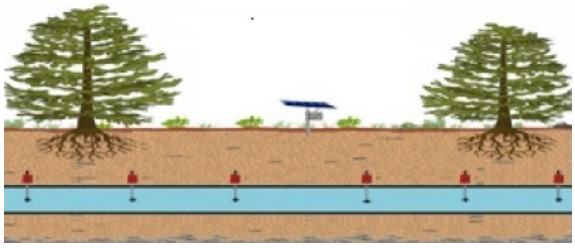

Figure 2.1: Example of WUN used in agriculture. [2]

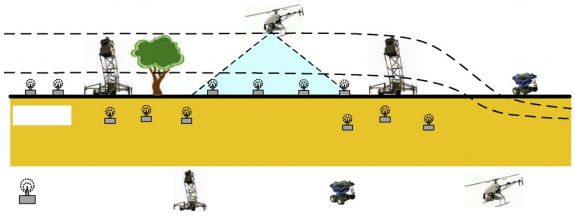

Figure 2.2: Hybrid wireless sensor network for border patrol. [3]

Compared to wired underground networks, WUN has some advantages: they are easier to deploy since the nodes don't require a physical connection with each other and they are harder to detect because there are no cables connecting the nodes.

2.2 Wireless Underground communication scenarios

In a wireless underground network there are buried nodes that communicate between them using the soil as propagation medium, but there are also aboveground nodes communicating with underground nodes. Here the propagation medium is hybrid (soil and air). Assuming bidirectional communication we will see that between a node aboveground and a node underground the link aboveground-underground is different from the link underground-aboveground and, for that reason we consider three different scenarios as we can see in the figure 2.3:

- **Underground-to-underground (U2U)** — Communication between two nodes when both of them are buried underground. In this scenario the propagation medium is always the soil. This scenario is used in multi hop underground networks;

- **Aboveground-to-underground (A2U)** — Communication between an aboveground node (the sender) and an underground node (the receiver). In this scenario the propagation

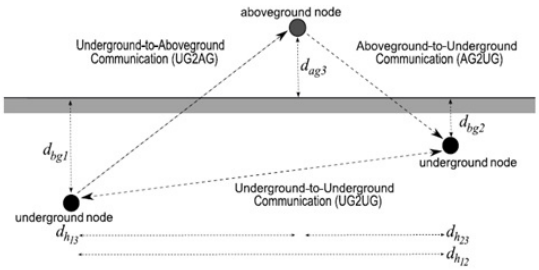

Figure 2.3: Types of communications in WUNs. [4]

medium is hybrid. This link is typically used to send control information to the underground nodes;

- **Underground-to-aboveground (U2A)** — On this link the underground node is the sender and the aboveground the receiver. The propagation medium is hybrid. This link is normally used to send the data measured to the aboveground data station that behaves as a data sink.

2.3 Underground channel models for WUNs

In this section we present the propagation models for the three different links referred in Section 2.2. Since the soil is a very different medium compared to the air we also present models to estimate its dielectric properties based on water content, percentage of sand and clay, and the frequency used for transmission. These models are important to estimate the parameters of the radio propagation models.

2.3.1 Dielectric soil properties model

In order to estimate the soil dielectric constant first we need to classify the kind of soil that we are using, by collecting a sample of the soil and analyse it in a laboratory to measure the percentage of sand, clay and silt. Based on these three parameters we can classify the soil using the texture triangle that is presented in the Figure 2.4.

Besides these three parameters the soil also has an amount of water which can be expressed as the Volumetric Water Content (VWC) that represents the fraction of water in the soil sample. The final input parameter for the dielectric model is the operating frequency.

In [14] the authors compare the Semi-empirical Mixing Dielectric Model (SMDM) proposed by Dobson and the Generalized Refractive Mixing Dielectric Model (GRMDM) in terms of their precision for determining the soil dielectric constant of not only the types of soils used to build the model but also other types of soils. They conclude that the SMDM model is not very accurate for types of soils other than those used to derive the model. The authors concluded that the GRMDM is more accurate than the SMDM when it comes to soil types that were not used to build the model.

The authors also present a model based on the GRMDM but with extra equations (Equation 2.9 to 2.17) to estimate some parameters that the GRMDM model requires to be measured. This

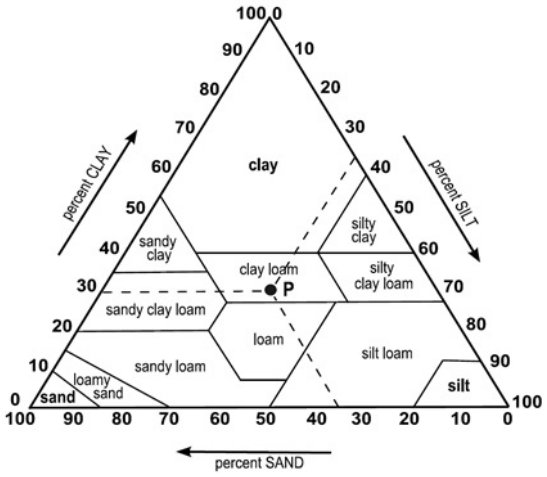

Figure 2.4: Soil texture triangle. [2]

model, named Mineralogy-Based Soil Dielectric Model (MBSDM), is described below and is the one we selected to be our model to estimate the soil dielectric constant. The selection is based on the simplicity of the SMDM model, which uses only the percentage of clay as input [14] and [15].

$$\varepsilon' = n_m^2 - k_m^2 \tag{2.1}$$

$$\varepsilon'' = 2 n_m k_m \tag{2.2}$$

According to this model the complex dielectric constant $\varepsilon = \varepsilon' - j\varepsilon''$ can be calculated using the Equations 2.1 and 2.2 respectively, where ε' is the dielectric constant and ε'' is the loss factor. The parameters n_m and k_m can be calculated as follows:

$$n_m = \begin{cases} n_d + (n_b - 1)m_v, & \text{if } m_v \leq m_{vt} \\ n_d + (n_b - 1)m_{vt} + (n_u - 1)(m_v - m_{vt}), & \text{if } m_v > m_{vt} \end{cases} \tag{2.3}$$

$$k_m = \begin{cases} k_d + (k_b - 1)m_v, & \text{if } m_v \leq m_{vt} \\ k_d + (k_b - 1)m_{vt} + (k_u - 1)(m_v - m_{vt}), & \text{if } m_v > m_{vt} \end{cases} \tag{2.4}$$

The parameters n_m, n_d, n_b, n_u and k_m, k_d, k_b, k_u are the values of the refractive index and normalized attenuation coefficient. The subscripts m, d, b, u stand for moist soil, dry soil, bound soil water and free soil water, respectively. m_v represents the Volumetric Water Content (VWC) and m_{vt} represents the maximum bound water fraction. The rest of the n and k parameters can be calculated using the following equations:

$$n_{d,b,u}\sqrt{2} = \sqrt{\sqrt{(\varepsilon'_{d,b,u})^2+(\varepsilon''_{d,b,u})^2}+\varepsilon'_{d,b,u}} \tag{2.5}$$

$$k_{d,b,u}\sqrt{2} = \sqrt{\sqrt{(\varepsilon'_{d,b,u})^2+(\varepsilon''_{d,b,u})^2}-\varepsilon'_{d,b,u}} \tag{2.6}$$

The $\varepsilon'_{d,b,u}$ are the real part of the dielectric constant of dry soil, bound water (physically bound with soil) and free water (moves in soil under gravity) respectively. The imaginary part of the dielectric constants are expressed with the $\varepsilon''_{d,b,u}$. This model also present expressions for calculating the dielectric constant for bound water and free water which are present next:

$$\varepsilon'_{b,u} = \varepsilon_\infty + \frac{\varepsilon_{0b,0u}-\varepsilon_\infty}{1+(2\pi f\tau_{b,u})^2} \tag{2.7}$$

$$\varepsilon''_{b,u} = \frac{\varepsilon_{0b,0u}-\varepsilon_\infty}{1+(2\pi f\tau_{b,u})^2}(2\pi f\tau_{b,u}) + \frac{\sigma_{b,u}}{2\pi\varepsilon_0 f} \tag{2.8}$$

The f is the wave frequency, the values of $\sigma_{b,u}$, $\tau_{b,u}$ and $\varepsilon_{0b,0u}$ are the conductivities, relaxation times and low frequency limit of dielectric constant for bound water and free water respectively. The GRMDM model uses the equations presented above from 2.1 to 2.8. With these equations we can estimate the dielectric properties of the soil we are considering, but for doing that we need the following soil parameters:

- Real (ε'_d) and Imaginary (ε''_d) parts of the complex dielectric constant for dry soil;
- Value of the maximum bound water fraction (m_{vt});
- Low frequency limits of dielectric constant for bound water (ε_{0b}) and free water (ε_{0u});
- Relaxation times for bound water (τ_{0b}) and free water (τ_{0u});
- Conductivities for bound water (σ_{0b}) and free water (σ_{0u}).

The value ε_0 is the dielectric constant for free space and ε_∞ is the high frequency limit which is equal to 4.9 for bound and free water.

Now that the GRMDM model was presented and we conclude that we need a significant number of parameters to use it, like, for example, the dielectric constant of the soil we are using without the presence of water (dry soil) we conclude that the model is not very easy to use when compared with the SMDM model proposed by Dobson, which requires only the sand and clay percentage of the soil.

After the analysis of this model and its requirements we will present next some equations that allow us to estimate the input parameters of the GRMDM model based only on the clay mass percentage (C) of the soil so that this model (named MBSDM) can be as easy to use as the SMDM [14].

$$n_d = 1.634 - 0.539 * 10^{-2}C + 0.2748 * 10^{-4}C^2 \quad (2.9)$$
$$k_d = 0.03952 - 0.04038 * 10^{-2}C \quad (2.10)$$
$$m_{vt} = 0.02863 + 0.30673 * 10^{-2}C \quad (2.11)$$
$$\varepsilon_{0b} = 79.8 - 85.4 * 10^{-2}C + 32.7 * 10^{-4}C^2 \quad (2.12)$$
$$\tau_b = 1.062 * 10^{-11} + 3.450 * 10^{-12} * 10^{-2}C \quad (2.13)$$
$$\sigma_b = 0.3112 + 0.467 * 10^{-2}C \quad (2.14)$$
$$\sigma_u = 0.3631 + 1.217 * 10^{-2}C \quad (2.15)$$
$$\varepsilon_{0u} = 100 \quad (2.16)$$
$$\tau_u = 0.5 * 10^{-12} \quad (2.17)$$

With the complex dielectric constant of the soil estimated ($\varepsilon' - j\varepsilon''$), plus the soil magnetic permeability (μ) we can determine the propagation constant $\gamma = \alpha + j\beta$, where the α is the attenuation constant and β is the phase constant, for a given angular frequency (ω), using Equations 2.18 and 2.19.

$$\alpha = \omega \sqrt{\frac{\mu\varepsilon'}{2}\left[\sqrt{1+\left(\frac{\varepsilon''}{\varepsilon'}\right)^2} - 1\right]}, \quad (2.18)$$
$$\beta = \omega \sqrt{\frac{\mu\varepsilon'}{2}\left[\sqrt{1+\left(\frac{\varepsilon''}{\varepsilon'}\right)^2} + 1\right]} \quad (2.19)$$

2.3.2 Underground-to-underground propagation model

The characterization of the underground channel is very important for designing new WUSNs and developing new protocols and mechanisms, such as new medium access control (MAC) optimized for underground communications. Here we present some models to estimate the underground-to-underground channel attenuation, which will then be used to create the ns-3 simulation model.

The simplest model is based on the Friis propagation model for free space and consists on taking into account the attenuation based only on the distance between the nodes. The Friis equation estimates the received signal strength at a distance d and can be written in the logarithmic form as follows [16]:

$$P_r = P_t + G_r + G_t - L_0 \quad (2.20)$$

where P_t is the transmission power, G_r and G_t are the gains of the receiver and transmitter antennas, respectively, and L_0 is the path loss in free space which is given by

$$L_0 = 32.4 + 20log(d) + 20log(f) \tag{2.21}$$

where d is the distance between sender and receiver and f is the operation frequency in MHz. For the propagation in soil we need to include a correction factor to take into account the soil medium, which adds some extra attenuation. As result the received signal strength equation is written as follow:

$$P_r = P_t + G_r + G_t - (L_0 + L_s) \tag{2.22}$$

where L_s is the additional path loss in the soil, calculated as follows:

$$L_s = L_\beta + L_\alpha = 154 - 20log(f) + 20log(\beta) + 8.69\alpha d \tag{2.23}$$

where β is the phase shifting constant and α the attenuation constant in soil.

The total path loss in dB for the direct propagation model can be expressed as follow:

$$\boxed{P_{sl}dB = 6.4 + 20log(d) + 20log(\beta) + 8.69\alpha d - 10log(G_a G_b)} \tag{2.24}$$

Using Equation 2.24 we can get an approximation of the attenuation in dBs between a sender and a receiver when both of them are buried. However, when estimating the total path loss in the underground channel we need also to take into account the reflecting wave that result from the underground surface, as shown in the Figure 2.5.

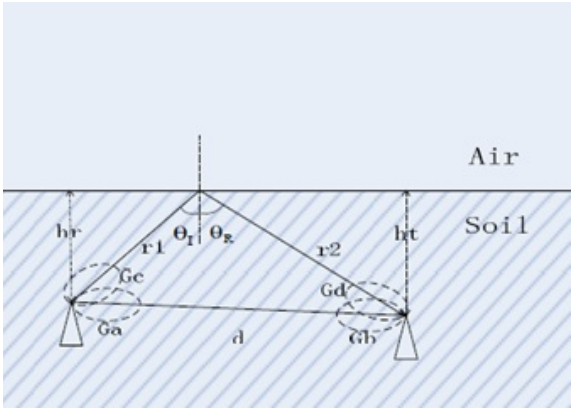

Figure 2.5: Two path channel model. [5]

This reflected wave has a greater effect when the buried depth of the nodes is lower, because in this case the reflected ray has a reduced distance to travel. For this reason, this signal component needs to be considered when estimating the path loss of the channel. The total path loss of the

channel considering the two-ray model can be computed using Equation 2.25 [5].

$$P_{fl}dB = P_{sl}dB - 10log\left|1 + \frac{\sqrt{G_cG_d}Rde^{\alpha\Delta r}}{\sqrt{G_aG_b}(r_1+r_2)}e^{-j\Delta\phi}\right|^2 \tag{2.25}$$

Where P_{fl} is the 2-ray path loss, G_c and G_d is the antennas gain in the r_1 and r_2 directions, respectively, $\Delta r = (r_1+r_2)-d$, $\Delta\phi = 2\pi(r_1+r_2-d)/\lambda$ and R is the reflection coefficient of the soil-air interface and can be calculated as follow:

$$R = \frac{\frac{1}{\varepsilon_r}\cos\theta_i - \sqrt{\frac{1}{\varepsilon_r} - \sin^2(\theta_i)}}{\frac{1}{\varepsilon_r}\cos\theta_i + \sqrt{\frac{1}{\varepsilon_r} - \sin^2(\theta_i)}}(perpendicularly - polarixed) \tag{2.26}$$

$$R = \frac{\cos\theta_i - \sqrt{\frac{1}{\varepsilon_r} - \sin^2(\theta_i)}}{\cos\theta_i + \sqrt{\frac{1}{\varepsilon_r} - \sin^2(\theta_i)}}(parallel - polarized) \tag{2.27}$$

As we can see from Equation 2.25 this new model take into account the buried depth of the nodes.

2.3.2.1 Underground-to-underground with lateral waves

In the section 2.3.2 we presented a propagation model that estimates the path loss of the underground channel by considering two fundamental waves of the propagated signal which are the direct wave that results from the line-of-sight between the two nodes and the reflected wave that results from the reflection on the soil-air interface. However, when the nodes are buried near the surface there is another wave that plays a major role in the propagation path loss between these two nodes which is named by the authors in [2] and [6] as the lateral wave. This new propagation model now includes three waves, named, the direct wave, the reflected wave and the lateral wave as we can see in the Figure 2.6.

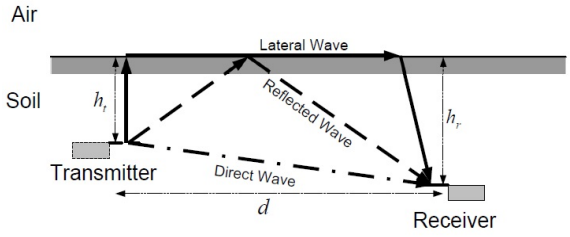

Figure 2.6: The three electromagnetic waves. [6]

As we can see from Figure 2.6 the lateral wave propagates in the soil, then goes to air and finally penetrates back into to soil. Since the attenuation in air is lower when compared to soil this wave will be the dominate component for lower depths and high horizontal distances.

From [6] the received power from each wave can be calculated by the following:

$$\boxed{P_d = P_t + 20log(\lambda_s) - 20log(r_1) - 8.69\alpha r_1 - 45} \quad (2.28)$$

$$\boxed{P_r = P_t + 20log(\lambda_s) - 20log(r_2) - 8.69\alpha r_2 + 20log(\Gamma) - 45} \quad (2.29)$$

$$\boxed{P_l = P_t + 20log(\lambda_s) - 40log(d) - 8.69\alpha(h_t + h_r) + 20log(T) - 30} \quad (2.30)$$

The P_t is the sender power, the λ_s is the wavelength in soil, the r_1 and r_2 are the distance travelled by the direct ray and the reflected ray respectively, d is the horizontal distance, α is the constant attenuation, Γ is the reflection coefficient and T is the refraction coefficient.

The reflection coefficient Γ is given by Equation 2.31, and the refraction coefficient T is given by Equation 2.32.

$$\Gamma = \frac{\frac{1}{n}cos\theta_{ri} - cos\theta_{rt}}{\frac{1}{n}cos\theta_{ri} + cos\theta_{rt}} \quad (2.31)$$

$$T = \frac{2cos\theta_{ri}}{n * cos\theta_{ri} + cos\theta_{rt}} \quad (2.32)$$

Where n is the refractive index of soil and θ_{ri} and θ_{rt} are the incident angle and refracted angle, respectively.

Now that we have the Equations for each one of the three components of the received power we need to combine those values in order to get a single value of the received power. This value can be estimated by the Equation 2.33.

$$\boxed{P_r = 10log(10^{\frac{P_d}{10}} + 10^{\frac{P_r}{10}} + 10^{\frac{P_l}{10}})} \quad (2.33)$$

This Equation 2.33 assumes the antenna gains equal to one.

2.3.3 Underground-to-aboveground propagation model

When building a WUSN we may also have aboveground nodes that can establish a bidirectional communication with underground nodes. The aboveground nodes may act as data sinks and/or as control stations. In this section we present a propagation model for the underground-aboveground communications link.

As we can see in the Figure 2.7 this situation differs from the underground-to-underground because now the propagated wave has to travel first in the soil, cross the soil-air interface, and then propagate in the air.

According to [17] and [18] the path loss can be calculated with the following equation:

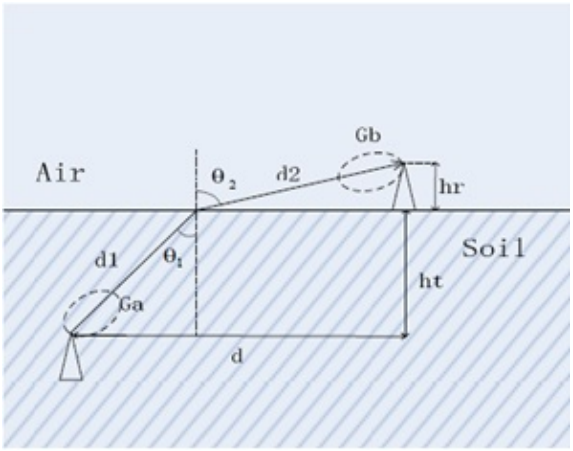

Figure 2.7: Underground-to-aboveground channel model. [5]

$$P_{u-a}dB = P_u dB + P_a dB + L_{ug-ag}dB \tag{2.34}$$

$$P_u = 6 + 20log(d_1) + 20log(\beta) + 8.69\alpha d_1 \tag{2.35}$$

$$P_a = 20log(f) + 20log(d_2) - 147.56 \tag{2.36}$$

$$L_{ug-ag} \approx 10log\frac{(\sqrt{\varepsilon'}+1)^2}{4\sqrt{\varepsilon'}} \tag{2.37}$$

As we can see in Equation 2.34 the path loss is a sum of three components where the first is the attenuation in the soil medium, the second is the attenuation in the air medium, and the third is the attenuation in the soil-air interface.

In the underground-aboveground path we need to be aware that the relative dielectric constant of soil is greater than the air. So, if the incident angle (θ_1) is larger than the critical angle ($\theta_c = arcsin(\sqrt{\frac{1}{\varepsilon_r}})$, ε_r is the real relative dielectric constant of soil) the ray will be completely reflected. Moreover, because the path in the air (d_2) is larger than the height of the aboveground node, the incident angle is approximately θ_c and the refracted angle approximately equal to 90^o. With these approximations we can estimate the distance travelled in soil and in the air, named, d_1 and d_2, respectively.

$$d_1 \approx \frac{h_t}{cos\theta_c} \tag{2.38}$$

$$dh_{soil} = \sqrt{d_1^2 - h_t^2} \tag{2.39}$$

$$dh_{air} = dh - dh_{soil} \tag{2.40}$$

$$d_2 = \sqrt{dh_{air}^2 + h_r^2} \tag{2.41}$$

These equations consider the propagation in U2A channel to be with an incident angle θ_c, but it is worth referring that in [19] the authors consider that the incident angle is approximately 0^o, which means that the distance travelled in soil is equal to h_u which is more accurate when

compared to the case A2U where all the authors [17], [18] and [19] agree that the distance travelled in soil is h_u. This is important to mention because if we consider that in the scenario U2A the angle is not 0^o the distance travelled in soil will be a little higher in this scenario when compared to the A2U, and consequently the attenuation will be higher for lower horizontal distances.

2.3.4 Aboveground-to-underground propagation model

This communication scenario is presented in the Figure 2.8. It is identical to the last one with the difference that this time we consider the link aboveground-to-underground.

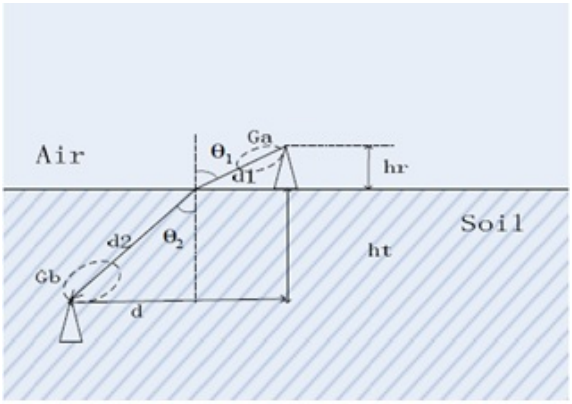

Figure 2.8: Aboveground-to-underground channel model. [5]

Since the propagation medium is air, air-soil interface and then soil, the equation that estimates the path loss is identical to the equation 2.34 presented in the last section and it can be written as follow:

$$P_{a-u}dB = P_a dB + P_u dB + L_{ag-ug}dB \tag{2.42}$$

$$P_a = 20log(f) + 20log(d_1) - 147.56 \tag{2.43}$$

$$P_u = 6 + 20log(d_2) + 20log(\beta) + 8.69\alpha d_2 \tag{2.44}$$

$$L_{ag-ug}dB \approx 10log\frac{(cos\theta_i + \sqrt{\varepsilon' - sin^2\theta_i})^2}{4cos\theta_i\sqrt{\varepsilon' - sin^2\theta_i}} \tag{2.45}$$

Now comparing Equations 2.42 and 2.34 we can see that they are basically identical. The only difference is that in the U2A link the interface is soil-air, which means that the ray goes from a higher refraction index to a lower refraction index. This leads to a lower attenuation than in the A2U scenario. In the U2A scenario total reflection can also occur, as we concluded in the early section.

The authors in [17] also did some approximations in order to estimate the distance travelled by the ray in each medium (d_1 and d_2). This approximations lead to the Equations 2.47 - 2.48.

$$d_2 \approx h_r \tag{2.46}$$

$$d_1 = \sqrt{h_t^2 + dh^2} \tag{2.47}$$

$$cos\theta_i = \frac{h_t}{d_1} \tag{2.48}$$

2.3.5 Aboveground-to-aboveground propagation model

As we can see in Figure 2.9 a complete WUN include nodes aboveground and underground that can communicate between them. This will force us to take into account the propagation over the air, which can be described by the Equation 2.49.

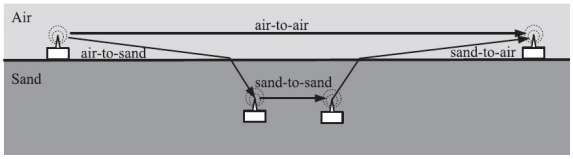

Figure 2.9: Communication scheme with multiple channel types. [7]

$$P_{a-a}dB = -147.56 + 20log(d_{air}) + 20log(f) \tag{2.49}$$

The Equation 2.49 assumes that the antenna gains are equal to 1, the frequency f is in Hz and the distance d_{air}, which is the distance in line of sight between the sender and the receiver, in meters.

2.4 Wireless underground networks using magnetic induction

As we already refer in Section 1.1 the soil communication medium vary with the weather conditions. This dynamic channel characteristic alongside with the high path loss in soil when compared to air makes it a very challenging scenario to use the well known Electromagnetic (EM) waves for wireless communication. So, as an alternative to EM communication that avoids these problems is the wireless communication using Magnetic Induction (MI).

In MI communications the signal transmission is done using two wire coils: one for the sender and another for the receiver, as we can see in Figure 2.10. For instance, if the transmitter coil has a current flowing through it with an angular frequency ω it will induce a current in the receiver coil that has the same frequency ω. This way, the wireless communication channel is established between the two coils.

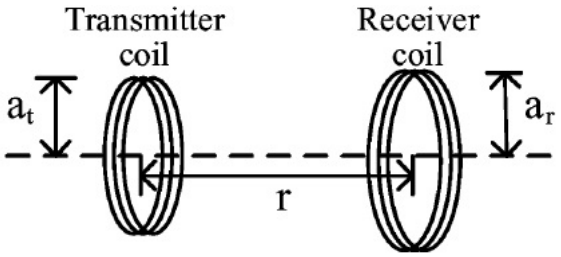

Figure 2.10: Magnetic induction channel. [8]

2.4.1 Magnetic induction propagation model

In [8], the authors derive an expression for the attenuation (P_r/P_t) in a MI channel. This expression is presented next as the Equation 2.50

$$\frac{P_r}{P_t} \approx \frac{\omega\mu N_r a_t^3 a_r^3 sin^2\alpha}{16 R_0 r^6} \tag{2.50}$$

The Equation 2.50 is only valid for the case where $(\omega\mu N_t \gg R_0)$. The parameters N_t and N_r are the number of loops in the transmitter and receiver coils, respectively; a_t and a_r are the radius of the transmitter and receiver coils, respectively; R_0 is the lower loop resistance; α is the angle between the axes of the two coupled coils, as we can see in Figure 2.11; r is the distance between the two coils and μ is the magnetic permeability of the environment where the coils are deployed.

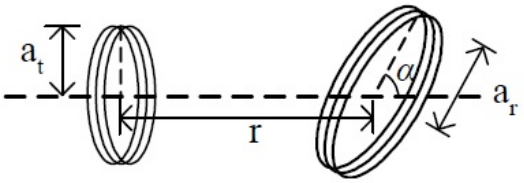

Figure 2.11: Angle between coils. [9]

One of the main advantages of the magnetic induction communication over electromagnetic waves in soil is the fact that in MI the only environment parameter that affects the attenuation is the magnetic permeability (μ), which means that for the MI the attenuation will be the same if the soil has low water content or high water content, because the magnetic permeability is the same in water and air. The Figure 2.12 compares the path loss of EM waves and MI system for different soil water content.

Although the MI system is insensitive to the water variation, the attenuation of this system is also very high as we would expect based on Equation 2.50, since the path loss is proportional to the factor $1/r^6$. Nevertheless in [8] the authors propose the use of relay coils, between the transmitter and the receiver, as we can see in Figure 2.13 to extend the communication range.

These relay coils allow the communication range to be extended considerably and, since they are passive elements, they do not require any power source and any processing power in oppose to electromagnetic relays. The principle is really simple, the sinusoidal current in the transmitter

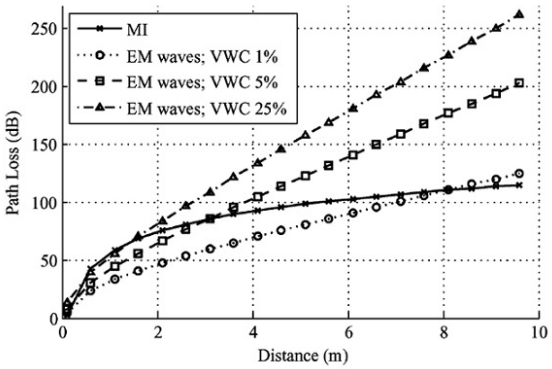

Figure 2.12: Path loss of EM wave in different soil water content and path loss in MI system. [8]

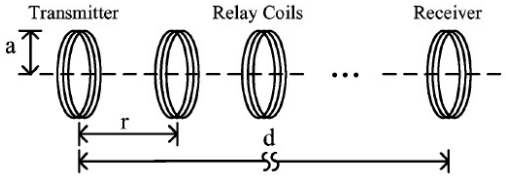

Figure 2.13: MI wave guide communication channel. [8]

coil induces a sinusoidal current in the first relay coil. Then, this relay coil is flowing by a current induced by the transmitter and it induces another current with the same frequency in the next relay coil. This goes on and on until the current reaches the receiver and, this way, we have a wave guide for the MI waves.

2.5 Wireless Underground Networks in mines and tunnels

When analysing wireless underground communications scenarios we can have another scenario which is the communication in a mine or a tunnel. In this case the communication medium is always the air, but the propagation characteristics of the EM waves is very different from those of the traditional aboveground communications, mostly due to the structure of the mine or the length of the tunnel and the dielectric properties of the walls.

There are also several mathematical models to describe this scenario and one of them is present in [1] and is named Multimode Model. This model is capable of characterizing completely the wave propagation on a tunnel in both near and far regions. However when we are dealing with caves the scenario can be different because in this case we need to consider the pillars that are disposed randomly. The multimode model overcomes this problem by combining their results with the shadow fading model in order to estimate the effects of reflections and diffractions suffered by the signal.

These networks have been the focus of many researches and are considered underground networks yet, since the medium is only the air they are out of scope for this MSc work.

2.6 Ns-3 Simulator

Ns-3, network simulator three, is an open-source discrete event network simulator targeted primarily for research and education purposes. It was written using the c++ programming language but the ns-3 library is wrapped to python thanks to the *pybindgen* library so if some users feels more comfortable with python they can use it instead of c++ to interact with the libraries.

The ns-3 is split into a couple of dozens of modules and each implement one or more models for real world network devices and protocols such as Wi-fi, WiMax, LTE for layers one and two and also several routing protocols such as OLSR and AODV.

When compared to other network simulators the ns-3 has some distinguishing high level design goals such as [20]

- **C++ and Python emphasis** — instead of use a domain specific modelling language to describe the models ns-3 uses the c++ or python languages;
- **Callback-driven events and connections** — simulation events in ns-3 are simply function calls that are scheduled to execute at a prescribed simulation time by use of a callback function as in contrast to specialized "handler" functions that centralize the processing of events in each simulation object;
- **Flexible core with helper layer** — ns-3 has a low level API that gives the users a lot of flexibility to configure the objects. However it also has some helper classes with some default configurations and easier to use functions;
- **Alignment with real-world interfaces** — ns-3 nodes, interfaces and objects such as sockets and net devices are aligned with those found in a Linux computer which improves the realism of the models and makes the comparison with real systems easier.

Since ns-3 is an open-source simulator and is widely spread over the research community and due to the lack of simulation models for underground communications these will be implemented and tested in this simulator during the realization of this MSc dissertation.

2.7 Summary

In this chapter we started by analysing some of the applications for WUNs and defined the communication scenarios that will be the targeted in this MSc work. Then, we presented some mathematical models for describing the soil properties and propagation characteristics in each of the three communication scenarios that will be simulated. For the propagation characteristics the main equations that are important to notice are: Equations 2.25 and 2.33 for the 2 rays model and U2U with lateral waves, respectively (U2U scenario); Equation 2.34 for the U2A link; and Equation 2.42 for the A2U link. For concluding the state of the art in wireless underground

networks we also introduced magnetic induction as an alternative to electromagnetic waves and refereed wireless networks in tunnels and mines because although they are beyond the dissertation objectives they still belong to the WUN group.

Since the main objective of this work is to implement the theoretical models into the ns-3 simulator we also went through an explanation of ns-3 and why we have chosen it. It is also important to notice that there is no simulation tool for these networks yet.

Chapter 3

Methodology

After identifying the main goal of the dissertation, which is to create a ns-3 accurate model capable of simulating wireless underground networks, and studying theoretical models for predicting the soil dielectric constant and signal attenuation, in this chapter we define the strategy used to create the ns-3 model and which of the literature experimental scenarios will be recreated in simulation environment for posterior ns-3 model validation.

3.1 Ns-3 propagation model details

The simulation model implemented should be able to predict the signal attenuation, the delay, throughput, jitter and the packet error ratio between two nodes in the cases of one or two buried nodes. Since the dielectric constant of the soil vary from one soil to another, based on the soil properties and volumetric water content, we identify another requirement for the model, which is, to estimate the complex soil dielectric constant based on the physical soil properties and the operating frequency of the nodes.

The class *ns3::TwoRayUndergroundModel* was created to implement the propagation model and the class *ns3::UndergroundConstantSpeedPropagationDelayModel* to implement the propagation delay model. In Figure 3.1 we can see the ns-3 architecture and the layer where our model fits, which is the propagation layer.

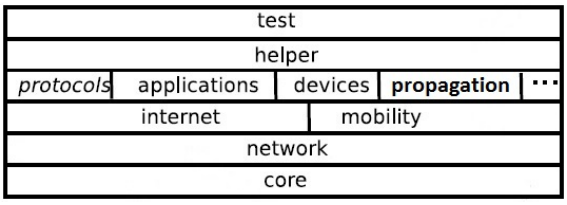

Figure 3.1: Ns-3 Architecture. [10]

For estimating the signal attenuation we used the mathematical equations presented in Chapter 2. The important equations for the underground channel that will be the used are: Equation 2.25 and 2.33 for the U2U communication, depending on if the user wants to use the two ray model

or the three ray model, respectively, Equation 2.34 for the U2A link and, Equation 2.42 for the A2U link. Since this model should be able to predict the signal attenuation in multi hop networks with several nodes buried and aboveground we also introduce the Equation 2.49 to include the case where there are two nodes aboveground that can reach each other. In this way our simulation environment is prepared for any kind of wireless underground network.

This model auto configures to the right scenario (U2U, A2U, U2A or A2A) based on the Z coordinate of each node, meaning that a node with a Z coordinate negative is buried in soil with depth -Z and a node aboveground is placed at a height Z (in meters). If only one of the nodes is buried it chooses scenario U2A if it is the sender node that is buried or A2U if it is the receiver node that is buried.

For the propagation delay estimation we created the class *ns3::UndergroundConstantSpeedPropagationDelayModel* which is based on the already implemented model *ns3::ConstantSpeedPropagationDelayModel* that considers the delay constant along the path between the sender and the receiver. It is important to notice that this existing model is only applicable to U2U links, since in those cases the electromagnetic wave will propagate exclusively in the soil. When one node is placed aboveground then we have to consider two propagation mediums, and this required the implementation of a new delay model. This delay model calculates the distance that the wave propagates in soil and uses the propagation speed in soil to measure the propagation delay, and then if the ray also travels in the air, it does the same calculations for the propagation in the air, using the vacuum speed of light. Then it sums the two delays and have the total delay between the two nodes.

An important property that is interesting to estimate when we are designing a new communication scenario is the packet error ratio. In ns-3 the model responsible to estimate it is the *ns3::NistErrorRateModel* by default. This model uses as an input to its calculations the power receiver sensitivity, the frequency, the modulation techniques (OFDM, DSS) and the forward error correction (FEC) codes used (if any).

Another important property that needs to be estimated is the complex dielectric constant, which is evaluated using the soil physical properties and the amount of water. In Chapter 2 we presented two models to calculate the dielectric constant, which are the SMDM model and the MBSDM model. With some analysis between experimental and theoretical results found in literature [14] we concluded that the MBSDM model is more accurate and so we focus on this model and implemented it in ns-3. However, due to the simplicity of adding another dielectric model to our implementation, and since the SMDM model is widely spread in literature, we decided to also include this model. By adding more than one mathematical model we give the user a chance to choose which model he wants to use to compute the dielectric constant. Since an user can already have estimated the soil dielectric constant, we decided to give the user the freedom to introduce manually the value of this constant directly in our ns-3 model instead of estimate it with one of the two models described above.

3.2 Simulation scenarios

Upon completing the implementation of the ns-3 propagation model presented in the Section 3.1 we validate the model by simulating the scenarios presented in the state of the art (U2U, A2U and U2A) for several soil types, depths of the buried nodes and lateral distance. The simulations are done using the 802.11 MAC, already implemented in ns-3, and the networks are tested in infrastructure mode.

The accuracy of the model for the 2.4 GHz frequency is evaluated by simulating the experimental scenarios described in [21] and comparing the practical results with the simulation results. The simulation tests output the received signal strength, delay, jitter, throughput and packet loss ratio (PLR).

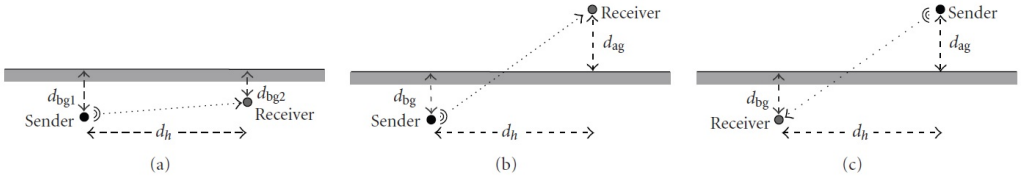

Figure 3.2: The basic simulation scenarios: (a) Underground-to-underground (U2U), (b) Underground-to-aboveground (U2A), (c) Aboveground-to-underground (A2U). [11]

To perform these simulations we create two nodes, where one of the nodes has the ns-3 *OnOff* application and the other one have the *DataSink* application. We did some modifications to the *DataSink* application in order to be able to collect the total number of bytes received so that we could measure the throughput of the link. For the collection of the PLR, delay and jitter we used the ns-3 tool *Flow Monitor* [22] that was developed at INESC. This tool is a monitoring module that automatically detects all the flows passing throw the network and collects the most important network metrics, such us number of received packets, packet loss, delay, jitter. For the last two, the *Flow Monitor* outputs histograms, so we estimated these metrics using the Equation 3.2 that calculates the average of the values in the histogram.

$$N = \sum_{i=0}^{M-1} H_i \tag{3.1}$$

$$\mu = \frac{1}{N} \sum_{i=0}^{M-1} C_i H_i \tag{3.2}$$

Besides the 2.4 GHz frequency we considered the 433 MHz frequency to validate the ns-3 propagation model. This is accomplished by replicating the experimental environment found in [2] for the U2U scenario and the [4] for the A2U and U2A scenarios. In this way we can measure the accuracy of our model for different frequencies and using different soil types.

3.3 Summary

In this chapter we presented the most important implementation details carried out upon the development of the simulation environment enabling the simulation of wireless underground networks. We started by gathering the main requirements of the model, which are the estimation of the signal attenuation, delay, packet error ratio, and the complex dielectric constant of the soil and then showed how they fit into the ns-3.

Since we also need to prove the accuracy of this model we defined some simulation scenarios that replicate experiments found in literature. After the simulations were performed we compare the results and conclude about the accuracy of the implemented model.

Chapter 4

Results

This chapter addresses all the simulation work that was carried out in order to validate our simulation environment. We start by first defining a simulation setup for the 2.4 GHz and then we present a comparison between the gathered results and the experimental results for both U2U and hybrid scenario (U2A and A2U). We also perform simulations for the 433 MHz in order to provide more than one source of validation. The chapter ends with a discussion on the results obtained.

4.1 Simulation setup

In this section we define some important parameters to simulate the experimental scenarios described in [21]. One of these parameters is the soil dielectric constant which varies with the soil water content and, also, from soil to soil. Table 4.1 shows the soil dielectric constant for the two soil types that were used in the experiments.

Soil Type	ε_r'	ε_r''
Loam	4.5	0.65
Sand	7.0	0.6

Table 4.1: Real and imaginary parts of the dielectric constant.

Having characterized the propagation medium where our simulations were carried out, we need to characterize the hardware that was used. During the field experiments [21] the transmission power was the maximum available, 20 dBm, and the carrier frequency used was 2.4 GHz. Although these experiments were performed by forcing the 802.11b and 802.11g rates we choose to carry out the simulations with the auto rate mechanism enabled. The used antennas have a gain of 2 dBi in transmitter mode and 3 dBi in receiver mode.

In order to simulate the network we created two simulation setups, one for estimating the throughput, and the other to estimate other metrics including delay, jitter, packet loss ratio and RSS. The reason for these two setups is that we need a simulation setup for measuring the delay, jitter and packet loss of the network when operating with typical data rates, in this case 1 Mbit/s,

and another setup for estimating the throughput which requires the nodes communicating at a higher data rate.

In the first setup to estimate the delay, jitter and packet loss ratio we did a simulation with two nodes using a data rate of 1 Mbit/s which we consider to be the normal data rate in these kind of networks (sensor networks). We set the simulation time to 50 seconds, but the transmitter was sending data for 30 seconds, in order to give more time so that the *flow monitor* can count all the lost packets. The simulations where repeated 50 times for each position of the nodes, using different seed numbers, so that we can have some variation of the results and then perform an average of the results.

In the second setup we estimate the maximum throughput of the network by placing two nodes side by side and then we choose the value 21 Mbit/s for the offered load, which is under the channel capacity (23 Mbit/s, according to our measurements) and perform the simulations to all the lateral distances until we reached a PLR above 50 percent. To achieve a reasonable sample we put the transmitter node sending data for 10 seconds, but we just stopped the experiment after 30 seconds so that the *flow monitor* could count all the lost packets. We performed this experiment for each position 20 times with different seed numbers so that we could make an average and estimate the throughput.

The simulations were carried out using 802.11 infrastructure mode in order to be closer to the experimental results that were also performed in this infrastructure mode. The chosen transport protocol was UDP because it has less overhead than TCP. The fact that with UDP we have less UDP makes easier to characterize the medium because in this way we avoid the constant TCP packets exchange that has a significant impact on the network performance.

Since we are measuring the accuracy of our model, at the end of every simulation setup we provide an error estimation of our model, comparing it with the experimental results. This error is calculated by doing the absolute difference between the two curves (the experimental and the simulated) and then estimating the average of those errors. By performing these estimations we can have an overview of how far are the estimated results from the real ones.

4.2 Underground-to-underground

In this section we presented the output of our simulations for the underground-to-underground scenario. These simulations were carried out using the two soil types presented in Table 4.1, with a 2.4 GHz frequency, and the results were obtained for different depths (10 cm and 40 cm depth in the loam soil; 20 cm and 40 cm depth in the sand soil) by varying the horizontal distance of the nodes.

4.2.1 Received Signal Strength

For the RSS we perform a simulation with the 2 ray model defined by the Equation 2.25 and another with the 3 ray model which is defined by the Equation 2.33. At the end of this section

we will also present the accuracy of our model in these simulations for each of the propagation models.

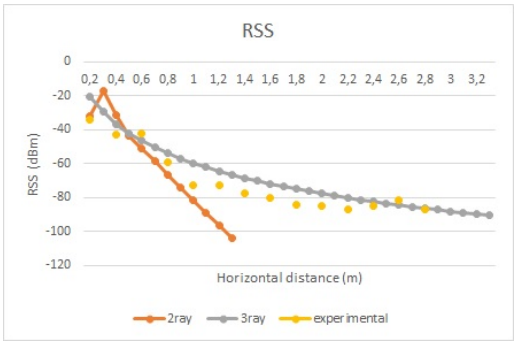

Figure 4.1: RSS at a depth of 10 cm.

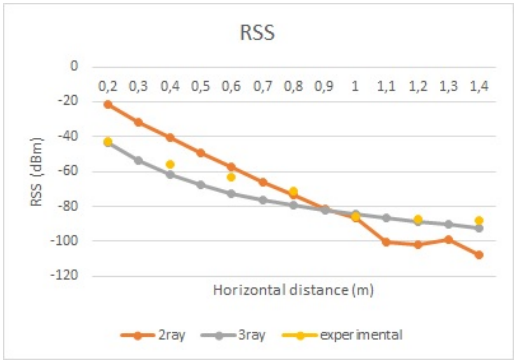

Figure 4.2: RSS at a depth of 40 cm.

From Figures 4.1 and 4.2 we can see the RSS results for the loam soil. We conclude that the 3 ray model is more accurate than the 2 ray model, specially in the 10 cm depth. Although in this case the 2 ray model does not predict the RSS for long horizontal distances it is still a good model for lower horizontal distances, approximately until 1 meter.

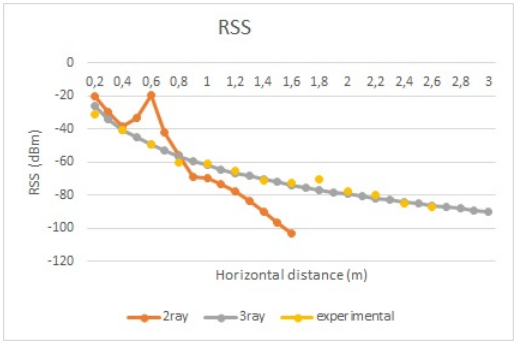

Figure 4.3: RSS at a depth of 20 cm.

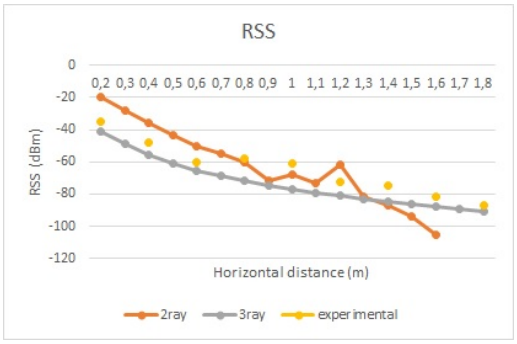

Figure 4.4: RSS at a depth of 40 cm.

In Figures 4.3 and 4.4 we display the same measures (RSS) as in Figures 4.1 and 4.2 but this time we used the sandy soil. Again, the 3 ray model is more accurate and the 2 ray model is only accurate for small horizontal distances, which leads us to conclude that the lateral waves are the dominant component of the signal in large distances. The fact that after 1 meter, approximately, the path loss decreased more slowly supports our hypothesis because the path loss over the air is much lower than in the soil.

Now that we have the results of our two models and compared each other, we measure the error of our simulation model, which is presented in Table 4.2.

The results presented in Table 4.2 are satisfying, since the higher error that we got was still less than 9 dBm (for the sand soil buried when the nodes were buried at 40 cm).

The Table 4.3 shows the communication range for the different scenarios. As we can see the accuracy of the predictions is higher for higher depths of the buried nodes. This can be explained due to the fact that the soil properties vary more horizontally in lower depths than in higher depths.

Depth (cm)	Loam	Sand
10	7.0	-
20	-	1.9
40	4.5	8.8

Table 4.2: Error in dB for the 3-ray model.

Setup	Simulated Range (m)	Experimental Range (m)	Error (m)	Relative Error (%)
Loam 10 cm	3.0	2.8	0.2	7.1
Loam 40 cm	1.2	1.2	0	0
Sand 20 cm	2.8	2.4	0.4	16.7
Sand 40 cm	1.6	1.8	0.2	11.1

Table 4.3: Real range vs estimated range.

In lower depths we can have vegetation, irregular surface, presence of other materials (e.g. rocks) and variation of water content. These variables are difficult to predict in simulation with precision and so, because we consider a regular surface at lower depths too is normal to have a higher error when compared to the experimental results.

4.2.1.1 Received Signal Strength for 433 MHz

After we performed an analysis of our RSS model for the 2.4 GHz frequency, in this section we perform another analysis but this time for the 433 MHz frequency. The output of this simulation will be compared with the experimental results obtained in [2] and [11].

Symbol	Description	Value
ρ_b	Bulk density	$1.33 g/cm^3$
ρ_s	Particle density	$2.66 g/cm^3$
S	Sand percentage	35%
C	Clay percentage	30%
m_v	Volumetric Water Content	15%

Table 4.4: Soil parameters of the experimental work.

Besides the soil properties characterized in Table 4.4, it is also important to refer that the transmitting power used was 10 dBm with an antenna gain of 0 dBi. Note that in this experiment the authors provide the soil properties but not the complex soil dielectric so we estimated it ourselves. Table 4.5 shows our dielectric estimative with both models presented in Section 2.3.1.

Model	ε_r'	ε_r''
SMDM	8.03	2.44
MBSDM	7.73	5.17

Table 4.5: Estimated real and imaginary parts of the dielectric constant.

Since the results presented in Table 4.5 revealed to be very different from one model to the other we choose to use both results and perform simulations with both models and compare the results produced by each model against the experimental results.

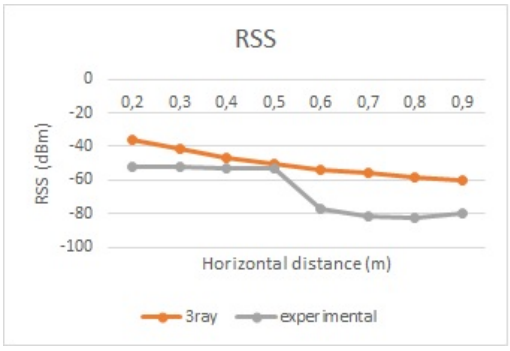

Figure 4.5: RSS for transmitted power at 10 dBm (SMDM).

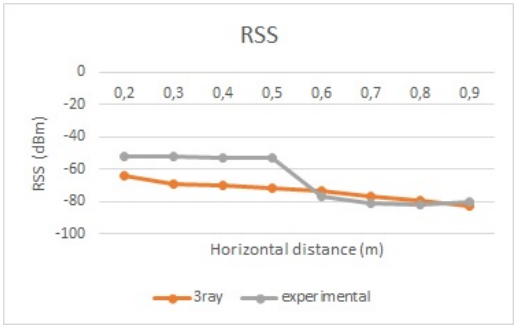

Figure 4.6: RSS for transmitted power at 10 dBm (MBSDM).

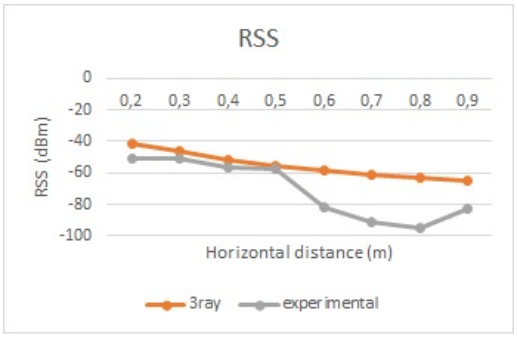

Figure 4.7: RSS for transmitted power at 5 dBm (SMDM).

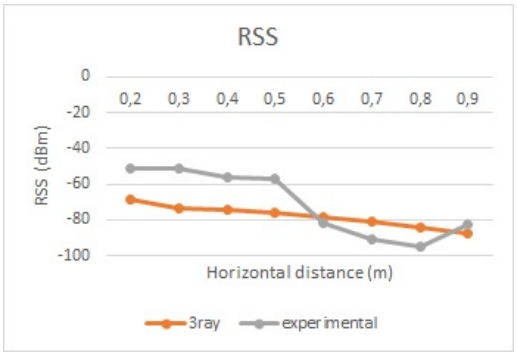

Figure 4.8: RSS for transmitted power at 5 dBm (MBSDM).

The Figures 4.5 and 4.6 shows a comparison between the simulated and the practical results for the case where the transmitted power was 10 dBm. We can see that, although the accuracy of the simulation is better for the case where we used the dielectric provided by the MBSDM model (at right), the simulated curve does not fit the experimental curve because they have a different shape. This can be explained due to the fact that the soil dielectric varies with the depth which is very difficult to take into account in a simulation environment. The same conclusions can be obtained from Figures 4.7 and 4.8 that represents the simulated experiment where the transmitted power was 5 dBm.

Now that we performed the simulations and briefly analysed the results it is time to estimate the error of our model, just like we did in Section 4.2.1 for the 2.4 GHz simulations.

As we can see from Table 4.6 the error obtained is higher when compared to the error obtained for the 2.4 GHz simulations (Table 4.2), but it is still satisfying if we use the soil dielectric constant provided by the MBSDM model. Unfortunately we do not have an exact value of the soil complex

Scenario	10 dBm	5 dBm
SMDM	16.01	15.51
MBSDM	9.55	13.3

Table 4.6: Error in dB for the 3-ray model.

dielectric constant in order to compare which soil model (SMDM or MBSDM) provided the most accurate dielectric values for this soil type.

4.2.2 Throughput

In order to carry out the throughput simulations we placed two nodes side by side and measured the maximum throughput that could be achieved using UDP. The absolute maximum throughput that we observed was approximately 23 Mbit/s. Since we wanted to measure the maximum throughput for different horizontal distances, we configured the *OnOff* application to transmit at a maximum of 21 Mbit/s of data. This is due to the fact that, as more distance we put between nodes lower is the channel capacity and so, in order to not saturate the channel while increasing the horizontal distance we configured the data generator *OnOff application* to transmit at about 90 % of the observed peak throughput. The simulations were performed by increasing the horizontal distances until we reached a PLR of about 50 %. Until this value we consider that we have an operating network.

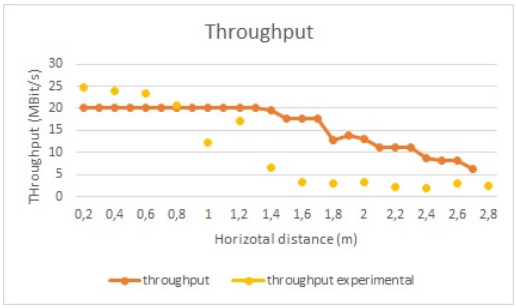

Figure 4.9: Throughput for loam soil at a depth of 10 cm.

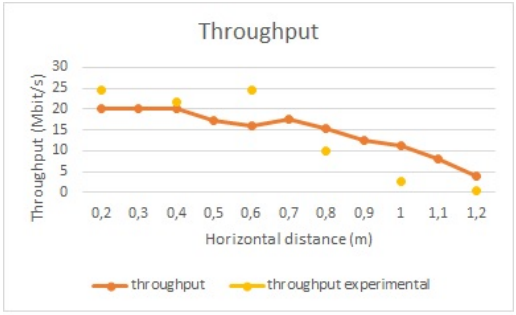

Figure 4.10: Throughput for loam soil at a depth of 40 cm.

After the analysis of the Figures 4.9 and 4.10 for loam soil we see that in the simulation the throughput stays almost constant for 1.4 m in the 10 cm depth setup and for 0.8 m in the 40 cm depth. In both cases the throughput then decreases as expected. This is due to the decrease of the SNR which leads to the increase of the bit error rate and, consequently, the packet error ratio. These same conclusions can be drawn for the sand soil as we can see in Figures 4.11 and 4.12.

From the Table 4.7 we conclude that our model in ns-3 is not very accurate to predict the throughput of the channel, specially for lower depths. This is due to the fact that for lower depths the experimental throughput drops much quicker than in the simulation. For example, for the loam soil at 10 cm depth the experimental throughput stays almost constant until we reach a lateral

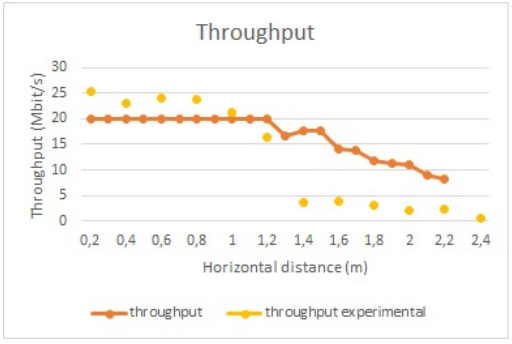

Figure 4.11: Throughput for sand soil at a depth of 20 cm.

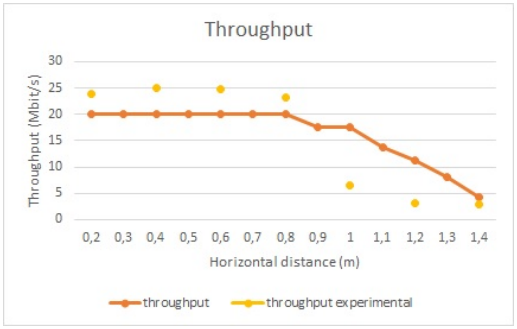

Figure 4.12: Throughput for sand soil at a depth of 40 cm.

Depth (cm)	Loam	Sand
10	6.5	-
20	-	6.2
40	5.3	5.3

Table 4.7: Error in Mbit/s for the throughput simulation.

distance of almost 0.8 m. In the simulation the throughput only drops at an horizontal distance of 1.7 m, which is almost the double horizontal distance. However, this effect was also observed for the 40 cm depth, the simulated results are more satisfying because we had a lower error.

4.2.3 Delay

In this section we study the communication delay in our network. This metric was evaluated in the field experiments with the *ping* command. So to try replicate the experiment in simulation environment we first tried to use the ns-3 *V4Ping* application, but since the results outputted by this application revealed to be very inaccurate and very unstable we decided to measure the delay of the network packets with the *flow monitor*. Although the round trip time (RTT) cannot be directly compared with the delay, we can assume, for the sake of simplicity, that RTT=2 * delay and conclude that both metrics give an overview of the network delay.

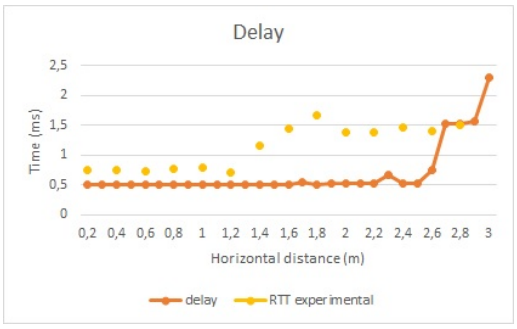

Figure 4.13: Delay in loam soil at a depth of 10 cm.

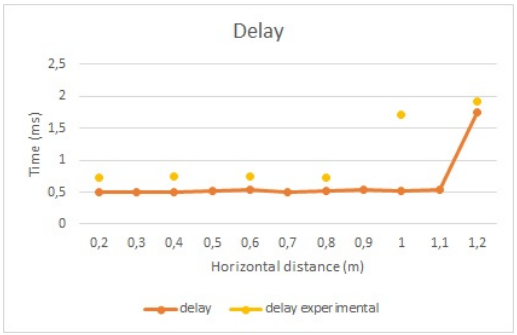

Figure 4.14: Delay in loam soil at a depth of 40 cm.

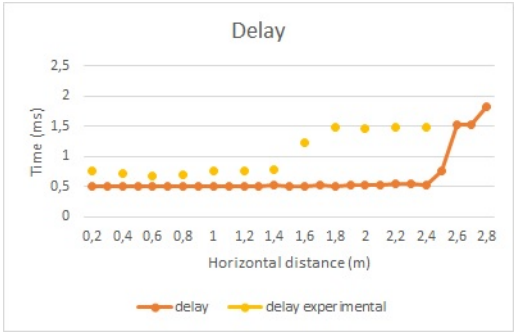

Figure 4.15: Delay in sand soil at a depth of 20 cm.

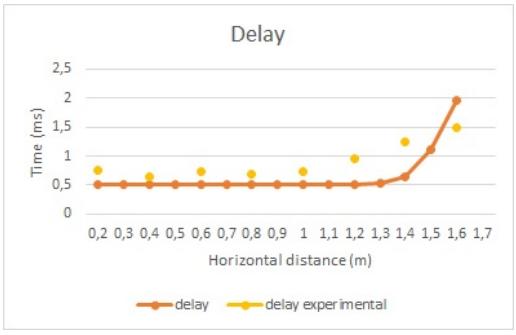

Figure 4.16: Delay in sand soil at a depth of 40 cm.

The Figures 4.13 and 4.14 compare the experimental round trip time and the simulated delay for the loam soil. Figures 4.15 and 4.16 give the same comparison for the sand soil. In these simulations we do not provide an error estimation because in simulation we used a metric (delay) different from that used in the real experiments (round-trip time). However, only by the graphics analysis we concluded that our model is not very accurate when it comes to predict the delay of our channel, mostly for lower buried depths (10 cm and 20 cm) because in these cases the delay stays low and constant for about 2.5m of horizontal distance, compared to the 1.2 m in the real experiments. For the 40 cm depth this distance is shortened to more or less 30 cm (1.2 m in the experimental results against 1.5 m in the simulated results), which leads to a higher accuracy for this depth.

4.2.4 Jitter

Our final metric for characterizing this network is the jitter, which is defined as the variation of the delay. Just like the delay, the jitter was obtained with the *flow monitor* tool from ns-3 in the case where the data rate of the *OnOff* application was set to 1 Mbit/s. This ns-3 application provides the module of the jitter, which means that the plots shows only positive values for this metric.

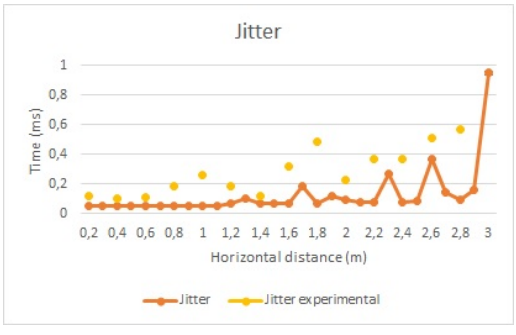

Figure 4.17: Jitter for loam soil at a depth of 10 cm.

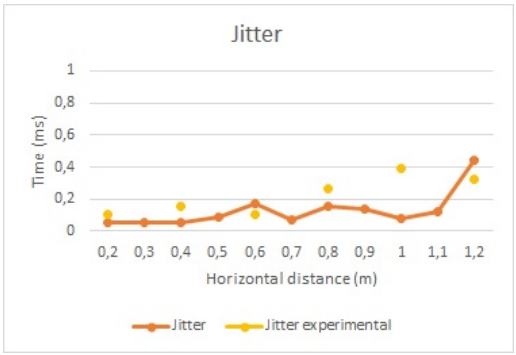

Figure 4.18: Jitter for loam soil at a depth of 40 cm.

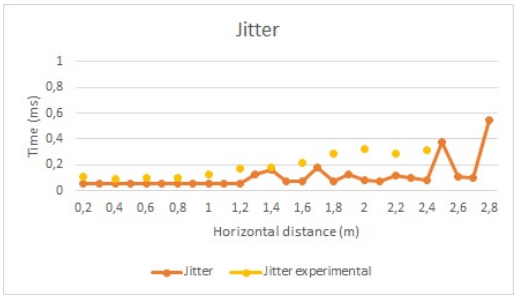

Figure 4.19: Jitter for sand soil at a depth of 20 cm.

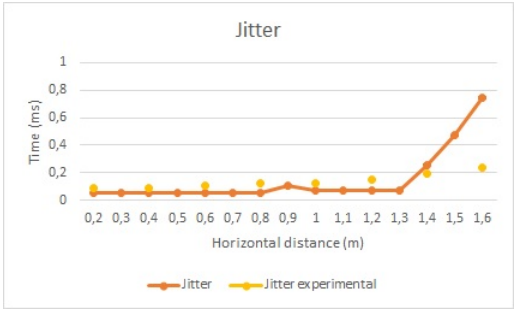

Figure 4.20: Jitter for sand soil at a depth of 40 cm.

The Figures 4.17 and 4.18 shows a comparison between the experimental and the simulated results for the loam soil. Figures 4.19 and 4.20 shows the same comparison for the sand soil. The Table 4.8 shows our model error. We can see that the model has less accuracy for the 10 cm depth, which was observed in Figure 4.17, because the jitter of the real experiment has a higher variation when compared to the other experiments, and our model was not able to follow this variation.

Depth (cm)	Loam	Sand
10	0.19	-
20	-	0.12
40	0.13	0.11

Table 4.8: Error in ms for the jitter simulation.

4.3 Underground-to-aboveground and aboveground-to-underground

The simulation results shown in this section represent the underground-to-aboveground and aboveground-to-underground. These simulations where performed in the same two soil types (sand and loam) as the other simulations, and using the same frequency (2.4 GHz). The results were obtained for different horizontal distances between the nodes, and placing the aboveground node at a fixed height of 1m, and the underground node at a depth of 40cm, just like in the experiments in [21].

As we did for the U2U simulations presented in Section 4.2, in this Section we will also provide results for the 433 MHz frequency.

4.3.1 Received Signal Strength

Here we compare the RSS experimentally measured with our simulations, for the 2.4 GHz frequency. The comparison between both results is presented in Figures 4.21 and 4.22 for the loam soil and sand soil, respectively.

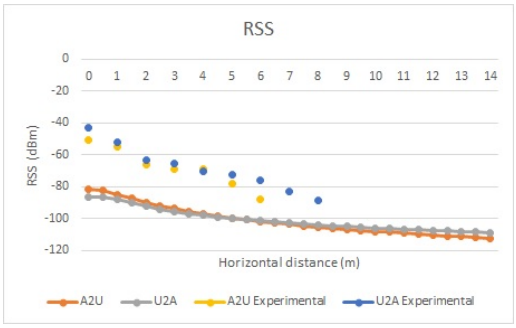

Figure 4.21: RSS for the loam soil.

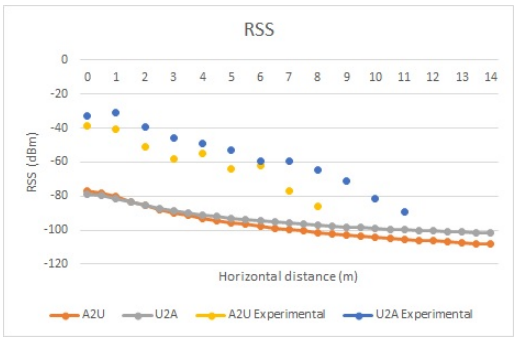

Figure 4.22: RSS for the sand soil.

With the analysis of these graphics we can conclude that the used model is not suitable for predicting the received signal strength in these hybrid scenarios. This conclusion is obtained by observing that in our model the received signal strength is about 40 dBm lower in the simulated results comparing to the experimental results for the first 2 meters in horizontal distance. Aside from that, we can also observe that the decay of our curve is about 25 dBm in 14 meters and the decay of the experimental curve is about 50 dBm, which is the double.

4.3.1.1 Received Signal Strength for 433 MHz

In Section 4.3.1 we concluded that our model is not adequate for the hybrid scenarios (soil plus air), but since we only performed simulations for one frequency we will do another simulation for the 433 MHz and analyse the obtained results that will be compared with the experiments done in [4].

In [4] the authors performed some experiments with one node buried at 15 cm or 35 cm and the other node was placed aboveground at a height of 2.5 m. The soil parameters where the experiments were conducted are defined in the Table 4.9.

Property	Value 0-20cm	Value 20-60cm
Bulk density	$1.33 g/cm^3$	
Particle density	$2.66 g/cm^3$	
Sand percentage	17%	16%
Clay percentage	28%	38%
Volumetric Water Content	9.5%	

Table 4.9: Soil parameters of the experimental work.

As we can see from Table 4.9 the soil is not uniform which means that its properties vary with depth. For the 15 cm simulations we have configured the parameters of 0-20 cm depth and for the 35 cm we configured the parameters for 20-60 cm depths. This last simulation is not very accurate since in this case the signal travels through the 0-20 cm depth before it reaches the surface, but we will ignore this in order to simplify the problem. The Table 4.10 shows the estimated complex soil dielectric constant using both dielectric models. Similarly to Section 4.2.1.1 we see, once more, that the estimated values vary a lot from one model to the other, but since we do not have the

actual values of our dielectric soil we have to use both models and compare the results with the experiments.

Model	ε_r'	ε_r''
SMDM15cm	4.75	1.43
MBSDM15cm	5.43	2.70
SMDM35cm	4.84	1.71
MBSDM35cm	5.073	2.47

Table 4.10: Estimated real and imaginary parts of the dielectric constant.

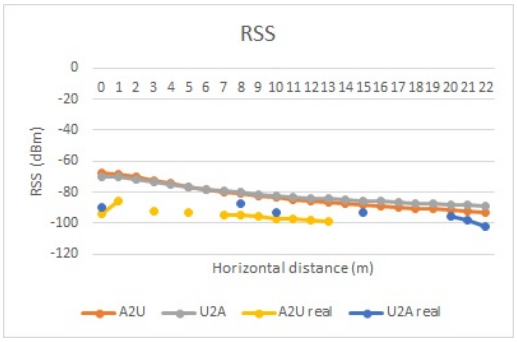

Figure 4.23: RSS for 35 cm depth (SMDM).

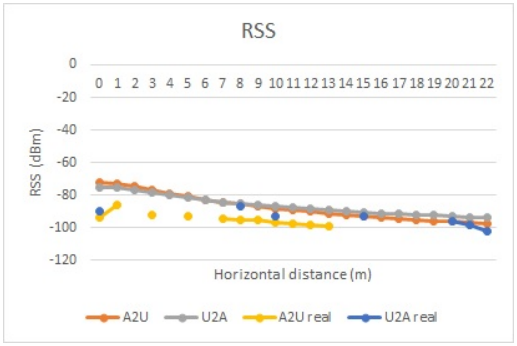

Figure 4.24: RSS for 35 cm depth (MBSDM).

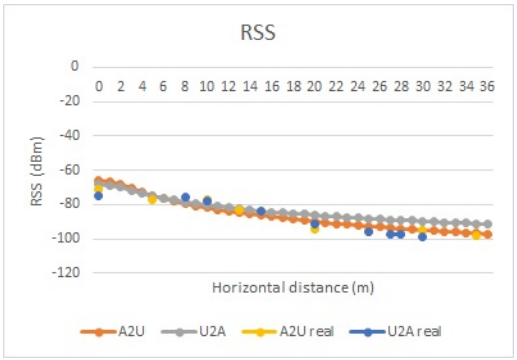

Figure 4.25: RSS for 15 cm depth (SMDM).

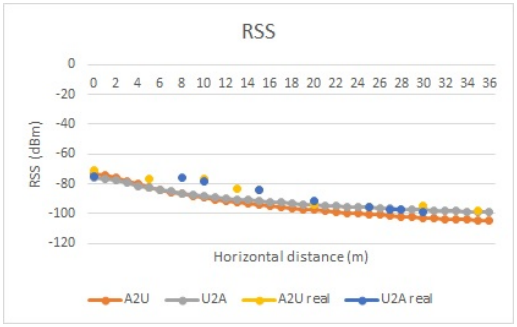

Figure 4.26: RSS for 15 cm depth (MBSDM).

The Figures 4.23 and 4.24 compare the experimental and the simulated results for the case where the buried node was placed at 35 cm depth. The Figures 4.25 and 4.26 shows the same compare but this time for the case where the node was buried at 15 cm. It is important to notice that the experimental results are surprising for the 15 cm depth, because in this case the authors obtained a higher attenuation in the U2A link which was not expected based on the theoretical models, and on the results of previous experiments in other setups.

Table 4.11 shows the estimated error for the simulations that were performed using the 433 MHz frequency. We observed that our model is more accurate for the 15 cm depth than it is for the 35 cm depth, which can be explained by the fact that this particular soil type has constant dielectric

Setup	A2U	U2A
MBSDM 15cm	6.8	3.7
SMDM 15cm	2.8	5.6
MBSDM 35cm	11.1	5.9
SMDM 35cm	15.8	19.1

Table 4.11: Error in dB for the hybrid model.

for the depth 0-20 cm and another for the 20-60 cm depth. Since our model only allows us to have one dielectric constant for the soil, we could not take this effect into account in our simulator.

4.4 Discussion

In the U2U case we can conclude that for higher depths, the attenuation is also higher, mostly because for higher depths the dominant signal component is the direct wave. For small depths, apart from the direct wave, we also have the reflected wave and the lateral wave. In this case we saw that this last wave is the dominant component after an approximate horizontal distance of 1 meter, since at 10 cm depth we observed that beyond the 1 meter distance the attenuation increases at a slowly rate with the increase of the horizontal distance. A similar conclusion can be drawn from the sand soil simulations at a depth of 20 cm. Because the lateral wave is the dominant component for high horizontal distances ($> 1m$) and lower depths ($\leq 20cm$) we also concluded that in this case the 2 ray model is not adequate which led us to use the 3 ray model. We also performed simulations with the intention to gather results about throughput, delay and jitter, and compared those results with the experimental results. Although these metrics were not very accurately predicted, the simulation could give us a rough estimate of these metrics. In general aspects we could conclude that our model has a higher accuracy for higher depths, specially when it comes to estimating the throughput, where we had an error of 6.5 Mbit/s for lower depths ($\leq 20cm$) comparing to an error of 5.3 Mbit/s for the higher depth ($40cm$). We observed the same results for the delay and jitter estimation. This is due to the fact that in real experiments the network conditions seem to deteriorate at about 1.2-1.4 m of horizontal distance and our model only starts counting that effect at about 1.8 m for the throughput and 2.4 m for the delay.

For the A2U and U2A communications we can conclude that the U2A link has a lower attenuation since the signal propagates from a high density medium to a lower density medium, meaning that the soil-air interface has lower losses when compared to the air-soil interface. We also showed that our model is not very adequate for the 2.4 GHz scenarios and, for this reason, we did not present results for throughput, jitter and delay because the results obtained were distinctively different from the experimental results. Nevertheless, we performed simulations for other scenarios where the frequency used was 433 MHz and in these simulations our model proved to be accurate, with the higher error being about 19 dBm if we consider the SMDM soil model or 11.1 dBm if we consider the MBSDM soil model. These higher errors, compared to the 15 cm depth can be explained by the fact that this particular soil type has one dielectric constant

for the 0-20 cm depth and another for the 20-60 cm depth and in the later case we only took into account the deeper dielectric constant which introduced some error in our model. Nevertheless, we could prove that our model is accurate for the 15 cm depth because the higher error was 6.8 dBm and the lower was 2.8 dBm which is minimum.

Chapter 5

Conclusion

This dissertation arises in the context of establishing wireless networks in the underground environment. These networks proved to be useful for monitoring in underground environments and they are definitely easier to deploy then their wired counterparts.

During our research we found some experiments for both MI and EM technologies, and also some theoretical propagation models. In this research material we also found out many challenges to overcome before successfully deploy a wireless underground network. Most of these challenges come from the type of medium we are using to communicate. The soil has a high attenuation and its dielectric properties highly depend of its soil type and the water contained, if we consider the EM waves.

Although the soil represents a difficult propagation medium there are more challenges to overcome and one of them is the complete lack of simulation tools for this environment. The main objective of this MSc thesis is to provide the first simulation tool for this kind of networks. The simulation framework that we developed allows us to easily design an underground wireless network and perform a quick simulation to adjust the distances between the nodes and estimate important parameters of the network. After the simulation is done the user gets a good estimative of what distance should be between nodes and with it the number of nodes that would be needed to cover the provided field. This is information very valuable when deploying, specially these kind of networks where the physical reachability of the nodes is reduced

5.1 Contributions

With the conclusion of this dissertation, and after we completed all the proposed goals, we achieved some important contributions. The first one is the complete study on wireless underground networks, including a deep study on the EM propagation models and soil dielectric estimation models. After this study we were able to create a simulation framework to estimate the major metrics in an underground network, the RSS, delay, jitter and throughput. After this tool was created we have validated it using several experimental scenarios and confronting these results with the ones obtained from our framework.

5.2 Future Work

The main improvements that can be done in order to push forward this investigation are the following:

- Perform more accurate field experiences using a laboratory and soil adapted antennas;
- Experimentally evaluate a multi hop network to compare with our simulator that already supports multi hop communication;
- Improve the hybrid (soil plus air) RSS model for the 2.4 GHz scenario;
- Propose new medium access protocols that take into account the soil propagation properties;
- Add the possibility of have a soil with different dielectric parameters for different depths, because the soil properties are not equal for all depths.

References

[1] Ian F. Akyildiz, Zhi Sun, and Mehmet C. Vuran. Signal Propagation Techniques for Wireless Underground Communication Networks. *Physical Communication*, 2(3):167–183, 2009.

[2] Agnelo R. Silva. *Channel Characterization for Wireless Underground Sensor Networks*. Thesis, 2010.

[3] Mehmet C. Vuran c Mznah A. Al-Rodhaan b Zhi Sun, Pu Wanga and Ian F. Akyildiz Abdullah M. Al-Dhelaan b. BorderSense: Border Patrol Through Advanced Wireless Sensor Networks. *Elsevier*, page 468–477, 2011.

[4] A.R. Silva Vuran. and M.C. Communication with Aboveground Devices in Wireless Underground Sensor Networks: An Empirical Study, 2010.

[5] Hu Xiaoya, Gao Chao, Wang Bingwen, and Xiong Wei. Channel Modeling for Wireless Underground Sensor Networks. *2012 IEEE 36th Annual Computer Software and Applications Conference Workshops*, pages 249–254, 2011.

[6] Xin Dong and Mehmet C. Vuran. A channel model for wireless underground sensor networks using lateral waves. *Global Telecommunications Conference (GLOBECOM 2011)*, pages 1–6, 2011.

[7] Pu Wang, Zhi Sun, Mehmet C. Vuran, Mznah A. Al-Rodhaan, Abdullah M. Al-Dhelaan, and Ian F. Akyildiz. On network connectivity of wireless sensor networks for sandstorm monitoring. *Computer Networks*, 55:1150–1157, 2010.

[8] Zhi Sun and Ian F. Akyildiz. Magnetic induction communications for wireless underground sensor networks. *IEEE TRANSACTIONS ON ANTENNAS AND PROPAGATION*, 58:2426–2435, 2010.

[9] Zhi Sun and Ian F. Akyildiz. Underground wireless communication using magnetic induction. *IEEE International Conference on Communications*, pages 1–5, 2009.

[10] Ns-3 Manual.

[11] Agnelo R. Silva Vuran and Mehmet C. Development of a Testbed for Wireless Underground Sensor Networks. *EURASIP Journal onWireless Communications and Networking*, page 14, 2009.

[12] I.F. Akyildiz, W. Su, Y. Sankarasubramaniam, and E. Cayirci. Wireless sensor networks: a survey. *Elsevier*, 38(4):393–422, 2002.

[13] D. Pompili E.P. Stuntebeck and T. Melodia. Wireless Underground Sensor Networks Using Commodity Terrestrial Motes, 2006.

[14] Lyudmila G. Kosolapova Valery L. Mironov and Sergej V. Fomin. Physically and Mineralogically Based Spectroscopic Dielectric Model for Moist Soils. *IEEE TRANSACTIONS ON GEOSCIENCE AND REMOTE SENSING*, 47:2059 –2070, 2009.

[15] Lyudmila G. Kosolapova Valery L. Mironov and Sergej V. Fomin. Correction to "Physically and Mineralogically Based Spectroscopic Dielectric Model for Moist Soils". *IEEE TRANSACTIONS ON GEOSCIENCE AND REMOTE SENSING*, 47:2085, 2009.

[16] Mehmet C. Vuran and Ian F. Akyildiz. Channel Model and Analysis for Wireless Underground Sensor Networks in Soil Medium. *Physical Communication*, 3(4):245–254, 2010.

[17] Zhi Sun and Ian F. Akyildiz. Connectivity in wireless underground sensor networks. *Sensor Mesh and Ad Hoc Communications and Networks (SECON)*, pages 1–9, 2010.

[18] Zhi Sun, Ian F. Akyildiz, and Gerhard P. Hancke. Dynamic connectivity in wireless underground sensor networks. *Wireless Communications*, 10(12):4334 – 4344, 2011.

[19] Xin Dong, Mehmet C. Vuran, and Suat Irmak. Autonomous precision agriculture through integration of wireless underground sensor networks with center pivot irrigation systems. *Ad Hoc Networks*, 11:1975–1987, 2013.

[20] ns-3. http://www.nsnam.org/, November 2013.

[21] José Oliveira. *Wifi Underground Wireless Networks*. Thesis, 2013.

[22] Gustavo Carneiro, Pedro Fortuna, and Manuel Ricardo. Flowmonitor - a network monitoring framework for the network simulator 3 (ns-3), 2009.